

1 **Can  $\delta^{18}\text{O}$  help indicate the causes of recent lake area expansion on the western Tibetan**  
2 **Plateau? A case study from Aweng Co**

3  
4 Yuzhi Zhang, Matthew Jones, Jiawu Zhang, Suzanne McGowan, Sarah Metcalfe

5  
6 Yuzhi Zhang

7 Key Laboratory of Western China's Environmental Systems (Ministry of Education), College of Earth and  
8 Environmental Sciences, Lanzhou University, Lanzhou, 730000, China

9 E-mail: zhangyzh15@lzu.edu.cn

10 ORCID ID: 0000-0003-4211-1780

11  
12 Matthew Jones

13 School of Geography, University of Nottingham, Nottingham, NG7 2RD, UK

14 E-mail: matthew.jones@nottingham.ac.uk

15 ORCID ID: 0000-0001-8116-5568

16  
17 Jiawu Zhang (✉)

18 Key Laboratory of Western China's Environmental Systems (Ministry of Education), College of Earth and  
19 Environmental Sciences, Lanzhou University, Lanzhou, 730000, China

20 E-mail: jwzhang@lzu.edu.cn

21  
22  
23 Suzanne McGowan

24 School of Geography, University of Nottingham, Nottingham, NG7 2RD, UK

25 E-mail: suzanne.mcgowan@nottingham.ac.uk

26 ORCID ID: 0000-0003-4034-7140

27  
28 Sarah Metcalfe

29 School of Geography, University of Nottingham, Nottingham, NG7 2RD, UK

30 E-mail: sarah.metcalfe@nottingham.ac.uk

31 ORCID ID: 0000-0003-1063-8940

32  
33 **Key words:** Lake sediment, Oxygen isotope, Water-balance model, Glacial melt water

34

35

36

37

38

39

40

41 **Abstract:** Glacier-fed lakes on the Tibetan Plateau (TP) have undergone rapid expansions since  
42 the late 1990s, concurrent with the changing climate. However, the dominant cause(s) of lake  
43 area increases is still debated. To identify the drivers of lake expansion, we studied Aweng Co,  
44 a glacier-fed lake in the western TP, where surface area has increased ( $0.74 \text{ km}^2 \text{ yr}^{-1}$ ) since the  
45 late 1970s and most rapidly ( $0.998 \text{ km}^2 \text{ yr}^{-1}$ ) since the late 1990s. A water balance model was  
46 used to clarify the reasons for increased lake water volume, supported by stable isotope  
47 hydrology and the  $\delta^{18}\text{O}$  change recorded in recent sediments. Results showed that glacial melt  
48 water probably had the biggest impact on changes in Aweng Co lake level in recent decades,  
49 but that precipitation was also an important contributor. Our study shows that  $\delta^{18}\text{O}$  of carbonate  
50 ( $\delta^{18}\text{O}_{\text{carb}}$ ) has great potential for indicating source changes of water supply in such lakes, but  
51 there is a need to be cautious when interpreting  $\delta^{18}\text{O}_{\text{carb}}$  due to the influence of multiple  
52 hydrological factors, which can change in dominance over time.

53

54

55

56

57

58

59

60

61

62

63

64

65

## 66 **Introduction**

67

68 Lake expansion (increased lake surface area) has been identified by remote sensing across the  
69 Tibetan Plateau (TP) in recent decades (Crétaux et al. 2016; Lei et al. 2013, 2014, 2017; Song  
70 et al. 2014; Zhang et al. 2015, 2017a). New lakes (99 larger than 1 km<sup>2</sup>) have appeared across  
71 the TP since 1970 and 81 % of the existing lakes have expanded, with a total increase in surface  
72 area of 7240 km<sup>2</sup> between the 1970s and 2010 (Zhang et al. 2017a). Most lakes in the inner TP  
73 have undergone an apparent increase in area since 1998 (Zhang et al. 2017a), verified both by  
74 satellite images and by ICESat altimetry measurements between 2003 and 2009 (Phan et al.  
75 2012; Song et al. 2013). Total water storage in 312 lakes (>10 km<sup>2</sup>) across the whole TP  
76 increased by an estimated 4.3 Gt from the early 1970s to 2000 and by 88.1 Gt between 2000  
77 and 2011 (Song et al. 2014).

78 The major factors leading to lake area increases have been identified as increases in  
79 runoff generated by more precipitation (Lei et al. 2014; Yang et al. 2014), glacier melt water  
80 (Yao et al. 2007, 2012) and permafrost thaw caused by higher temperatures (Yang et al. 2010).  
81 However, the impacts of climatic drivers on lake water balance are complex, often  
82 interconnected, and variable across the interior TP. Lakes in different regions of the TP are  
83 recharged by different sources of water including rainfall, snowfall, glacier melt water and  
84 groundwater. In the central, northern, and northeastern TP, lake levels increase during the warm  
85 season and decline in the cold season, related to annual changes in monsoonal precipitation and  
86 evaporation (Lei et al. 2017). In the northwestern TP, however, lake levels increase both in  
87 spring (March to May) and in summer (June to August); this is closely linked to increased  
88 snowfall in spring and glacier melt in summer, which currently accounts for 30-40 % of total  
89 annual precipitation (Lei et al. 2017).

90 Water balance models based on meteorological data, are an efficient way to investigate  
91 the effects of climate change on hydrological processes for water resource planning (Gleick  
92 1987; Guo et al. 2002; Rouse 1998; Song et al. 2014). These models have been widely used for  
93 estimating the relative importance of hydrological sources and sinks (Conway 1997; Xu et al.  
94 2020; Zhu et al. 2010) and predicting consequences of future changes in streamflow (Atkinson

95 et al. 2002). Such models have, however, only previously been applied to six lakes located in  
96 the central TP (Lei et al. 2013; Zhu et al. 2010) where hydrological controls are largely  
97 monsoonal-driven. Less is known of hydrological processes in the western TP. Lake sediment  
98 records are widely used for studying regional hydrological variations, such as lake level changes  
99 (Magny 2004; Qiang et al. 2013; Rowe et al. 2003). Combining water balance models based on  
100 instrumental datasets with palaeolimnology is a potentially powerful validation approach for  
101 understanding the drivers of lake change.

102         Given the multiple potential drivers of lake level change, a lake-by-lake rather than a  
103 regional conceptual model approach is needed for down core interpretations of hydroclimatic  
104 change. Here we present a detailed study of lake area change since the late 1990s from an alpine  
105 lake, Aweng Co in the western TP. The lake is hydrologically closed, fed by direct precipitation  
106 onto the lake surface, and runoff generated by precipitation and glacier melt water. In order to  
107 identify the dominant factors that led to lake area expansion, we analysed the components of a  
108 water balance model that could influence lake water volume change since the late 1990s,  
109 including the use of  $\delta^{18}\text{O}$  as a tracer. We then compared the  $\delta^{18}\text{O}_{\text{carb}}$  values in recent sediments  
110 with the water balance model to verify the water supply variations, and to understand the  
111 relationship between the water source changes and changes in the  $\delta^{18}\text{O}_{\text{carb}}$ . This aim of the study  
112 is to improve our understanding of the factors controlling lake system change in such  
113 environments, over both recent and palaeo-timeframes.

114

## 115 Study Site

116

117 Aweng Co (A'ong Co, 32.70° ~ 32.82° N, 81.63° ~ 81.80° E) is a closed-basin saline lake  
118 located in the western Tibetan Plateau (Fig. 1a). It lies at 4,430 m a.s.l. and is surrounded by  
119 500 m high hills. Catchment vegetation, where present, is typical of alpine desert steppe  
120 including *Stipa* grasses. The catchment mainly consists of Cretaceous granite and Jurassic  
121 metamorphosed sandstone. Aweng Co is an elongated, shallow lake, which is 23.4 km long with  
122 a mean and maximum width of 2.52 km and 5.30 km respectively; the maximum water depth  
123 is 6 m. Within a large catchment area (2052.30 km<sup>2</sup>), the current lake water area is only 68.96

124 km<sup>2</sup> (in 2015). In the western part of the catchment, glaciers and snow at elevations higher than  
125 5000 m a.s.l (Fig. 1b) cover an area of 125.80 km<sup>2</sup> (Li et al. 2017; Song et al. 2014; Wang et al.  
126 1998), and are currently approximately 50 km from the lake. Satellite imagery shows that the  
127 lake area expanded dramatically from the late 1990s (ESM 1).

128 In 2015 a pH of 9.2 and salinity of 29.5 g L<sup>-1</sup> were recorded in the lake centre, with  
129 concentrations of 1850 mg L<sup>-1</sup> CO<sub>3</sub><sup>2-</sup> and 2023 mg L<sup>-1</sup> HCO<sub>3</sub><sup>-</sup>. Meteorological data at the  
130 Shiquanhe Station (32.50° N, 80.08° E; altitude: 4279.3m a.s.l.), 150 km from Aweng Co, show  
131 that mean annual temperature and total precipitation are 0.68 °C and 69.11 mm (for the period  
132 1971-2012, <https://data.cma.cn/>). 87.6 % of precipitation at Shiquanhe falls between May and  
133 September during the Indian Summer Monsoon (ISM) season (Fig. 1c). The mean temperatures  
134 in January and July are -12 °C and 14 °C, respectively. Monthly mean temperature is above  
135 0 °C between May and October (Fig. 1c), and the lake surface usually freezes in October and  
136 thaws in May. The δ<sup>18</sup>O value of the central lake waters was 0.2 ‰ in 2015.

137

## 138 **Materials and Methods**

139

### 140 **Lake volume reconstruction**

141

142 The region has been monitored by satellite imagery since the 1970s, including Landsat 4-5  
143 Thermal Mapper (TM), Landsat 7 Enhanced Thematic Mapper (ETM), and Landsat 8  
144 Operational Land Imager (OLI). Lake area data from the National Tibetan Plateau Data Center  
145 (<http://data.tpdc.ac.cn/>; Zhang et al. 2014, 2019a; Zhang 2019) is averaged over 3 or 4 years,  
146 and so is of insufficient resolution to determine annual changes in lake area. Therefore, we used  
147 images with no cloud cover from the Geospatial Data Cloud (<http://www.gscloud.cn/>; ESM 2),  
148 sampled at a consistent time of the year (September - October) to minimize the influence of  
149 seasonal variability (Zhang et al. 2017b). This period is useful for comparing inter-annual  
150 changes in lake area because it records lake size at the end of the warm and wet season. Gaps  
151 in the Landsat ETM+ scan line corrector-off images were filled by the neighbourhood similar  
152 pixel interpolator algorithm (Chen et al. 2011). Lake area data before 1990 was downloaded

153 from the National Tibetan Plateau Data Center (Zhang et al. 2014, 2019a; Zhang 2019).

154 We calculated past changes in lake volume using a combination of the lake area  
155 measurements and a digital elevation model (DEM) of the lake, derived from a bathymetric  
156 survey by SM-5A hand-held sonar conducted in 2015. Lake volume was calculated using the  
157 VOLUME function in Surfer 11.0 sequentially lowering lake levels. Lake level altitude data  
158 was derived from ICESat Laser altimetry measurements, which were available from 2003 to  
159 2009 (Zhang et al. 2011, 2017a). We calculated the lake level altitude for 1999 ~ 2002 and 2015  
160 and thereby lake volume, according to the correlation between lake area and lake-level altitude  
161 from 2003 to 2009. The lake volume before 1999 was calculated from this relationship using  
162 lake area measurements from the National Tibetan Plateau Data Center (Zhang et al. 2014,  
163 2019a; Zhang 2019).

164

165 Stable isotopes of water and sediments

166

167 In 2015, a 411.5 cm long sediment core (AWC2015B) was taken from the central part of the  
168 lake (32.75° N, 81.76° E) at a water depth of 6 m using a UWITEC corer (Fig. 1b). The  
169 chronology of the core top was established by  $^{137}\text{Cs}$  and  $^{210}\text{Pb}$  using HPGe Gamma  
170 Spectrometry.  $^{210}\text{Pb}$  was obtained via gamma-emission at 46.5 keV and  $^{226}\text{Ra}$  at 351.92 keV  $\gamma$ -  
171 rays emitted by its daughter isotope  $^{214}\text{Pb}$ . The age of the top sediment was established by the  
172 Constant Rate of Supply (CRS) model (Appleby and Oldfield 1978). The top 14 cm, which  
173 covered the period with instrumental data, was used in this study, with a sampling interval of  
174 0.5 cm.

175 Fine-grained carbonates (<40  $\mu\text{m}$  fraction) were collected from sediments by wet  
176 sieving and then dried at 50 °C for 6 hours. The minerogenic composition was confirmed to be  
177 aragonite by X-ray diffraction analysis. Stable oxygen isotopes were analysed from the  
178 carbonates using a ThermoFisher MAT 253 mass spectrometer with an automated carbonate  
179 preparation device (Kiel IV). Four standards (NBS18, NBS19, GBW04406, GBW04405) were  
180 measured every 10 samples. Analytical precision for  $\delta^{18}\text{O}$  and  $\delta^{13}\text{C}$  was better than 0.1 ‰.  
181 Values were reported relative to the Vienna Pee Dee Belemnite (VPDB) standard. All the

182 measurements were carried out in the Key Laboratory of Western China's Environmental  
183 Systems, Lanzhou University.

184 During the field season (in July 2015) a number of lake water and precipitation samples  
185 were taken from the lake and catchment to better understand the isotope hydrology of the lake  
186 system. Lake water and a groundwater sample from a catchment spring were filtered using a  
187 syringe filter with 0.45- $\mu\text{m}$  membranes and then hermetically stored in a 5 mL polyethylene  
188 bottle. Rainfall samples were also collected and sealed in a 5 mL polyethylene bottle. Falling  
189 snow was collected in a clean stainless steel bowl, which melted quickly as it was at the end of  
190 June, and the resulting water was then transferred into a 5 mL polyethylene bottle. All the water  
191 samples were stored at 4 °C before analysis. Stable isotopes of all the samples were measured  
192 by an Isotopic Liquid Water Analyzer (Picarro L1102-i) at Lanzhou University. The values are  
193 reported relative to the Vienna Standard Mean Ocean Water (VSMOW) standard. Analytical  
194 precision for  $\delta^{18}\text{O}$  and  $\delta^2\text{H}$  was better than 0.1 ‰ and 0.3 ‰, respectively.

195

#### 196 Hydrological model

197

198 To begin to identify the likely contributions of hydroclimate, such as evaporation, precipitation,  
199 and glacial melt water, to the observed increase in Aweng Co lake area over recent decades, we  
200 attempted to model the lake hydrology based on equation 1. We made the assumption that  
201 volume changes at Aweng Co are controlled by a number of inputs and outputs to the system  
202 (Equation 1), recognising that there is no surface outflow from the lake.

$$203 \Delta V_L = P_L S_L + R_C S_C + GMW + G_I - E_L S_L - G_O \quad (1)$$

204 where  $\Delta V_L$  is the change in lake volume ( $\text{m}^3$ ) in a given time,  $P_L$  is the precipitation onto the lake  
205 surface,  $S_L$  is the lake surface area;  $R_C$  is runoff from the catchment;  $S_C$  is the catchment area  
206 excluding the lake area;  $E_L$  is the total evaporation on the lake surface;  $GMW$  is the glacier melt  
207 water and  $G_I$  and  $G_O$  are inflow and outflow groundwater components respectively. Because the  
208 lake area of Aweng Co expanded dramatically since the late 1990s, we employed the water  
209 balance model for the period of 1999-2009 in this study.

210  $\Delta V_L$ , the change in lake volume, is a known value, as are the lake and catchment areas

211 from the remote sensing work. Because there is no meteorological station in the study area,  
 212 precipitation in the Aweng Co basin was taken from the LZU0025 dataset (Wu et al. 2014)  
 213 calculated using the Thin Plate Smoothing Spline (TPSS) method which interpolates data from  
 214 all meteorological stations in China. Due to the positive correlation between precipitation and  
 215 elevation in the western Tibetan Plateau (Zhang et al. 2019b), the interpolated precipitation  
 216 values in the Aweng Co catchment (Table 1) are higher than those from Shiquanhe Station. The  
 217 quantity of the precipitation falling on the catchment that reaches the lake is unknown, and is  
 218 probably a combination of surface and groundwater, or at least sub-surface flow. Here we take  
 219 overland flow ( $R_c$ ) to be a proportion ( $c$ ) of precipitation falling on the catchment.

220 Glacial melt water may reach the lake through both overland and sub-surface flow. Here  
 221  $GMW$  is taken to be the surface component, such that  $GMW$  is estimated based on the measured  
 222 change in glacial volume available for the Aweng Co catchment, multiplied by a constant ( $g$ ).  
 223 To convert measured glacial area ( $S_g$ ) to a volume ( $V_g$ ) we used the formula from Zhu et al.  
 224 (2010) based on data from 253 glaciers in the China Glaciers Catalogue,  $V_g = 0.042S_g^{1.3565}$ .  
 225 Variation in glacier volume was converted to glacier melt water volume by multiplying by 0.85  
 226 (Huss 2013), and only 42 % of this volume is known to drain into the Aweng Co basin (Neckel  
 227 et al. 2014). Unknown constants  $c$  and  $g$  both therefore take into account potential infiltration  
 228 and evapotranspiration, i.e. factors that prevent all precipitation or melt water flowing directly  
 229 into the lake.

230  $E_L$  (mm day<sup>-1</sup>) is calculated using the equation of Linacre (1992) such that  
 231 
$$E_L = [0.015 + 4 \times 10^{-4}T_a + 10^{-6}z] \times [480 \frac{(T_a+0.006z)}{84-A} - 40 + 2.3u (T_a - T_d)] \quad (2)$$
  
 232 where  $T_a$  is air temperature (°C),  $z$  = altitude (m),  $A$  = latitude (degrees),  $u$  = wind speed (m  
 233 s<sup>-1</sup>),  $T_d$  = dew point temperature =  $0.52T_{a\ min} + 0.60T_{a\ max} - 0.009(T_{a\ max})^2 - 2$  °C. This has  
 234 been shown to be a reasonable estimate of evaporation where full suites of meteorological data  
 235 are not available (Jones et al. 2016). Because data for  $T_{a\ min}$ ,  $T_{a\ max}$  and  $u$  are unavailable in  
 236 the LZU0025 dataset, they were taken from the National Centers for Environmental Prediction  
 237 (NCEP)-Department of Energy (DOE) Reanalysis 2 Gaussian Grid data  
 238 (<https://www.esrl.noaa.gov/psd/data/gridded/data.ncep.reanalysis2.gaussian.html>). When  
 239 calculating the precipitation and evaporation on the lake surface, we used the mean lake area



240 for the measurement year, estimated from the lake area at the beginning and end of each year.  
 241  $G_i$  and  $G_o$  are unknown.

242 To investigate the remaining unknowns in the lake hydrology model we firstly aimed to  
 243 optimize calculated changes in lake volume, using equation 1, with those that have been  
 244 measured. As a first order test, we aimed to optimize values of  $c$  and  $g$  such that these constants  
 245 are  $\geq 0$  and the regression relationship between known and modelled  $\Delta V_L$  has a slope and  $r^2$  of  
 246 1 and an intercept of 0.

247 We then took an index lake approach (Gibson et al. 2016; Jones et al. 2016) to  
 248 understand whether the lake is likely to have any groundwater outflow. This approach calculates  
 249 the isotopic composition of the theoretical lake ( $\delta_L$ ) that sits at the extreme end of the local  
 250 evaporation line (LEL) i.e. a fully closed hydrological system where  $P\delta_P = E\delta_E$ . As  $\delta_E$  is a  
 251 function of  $\delta_L$ , and in the case of the index lake  $\delta_E = \delta_P$ ,  $\delta_L$  can be calculated. We use the  $\delta_E$   
 252 equation based on the Craig-Gordon Evaporation model (Craig and Gordon 1965), as used by  
 253 Steinman et al. (2010a, b):

$$254 \quad \delta_E = \frac{\alpha^* \delta_L - h \delta_A - \varepsilon}{1 - h + 0.001 \varepsilon_k} \quad (3)$$

255 where  $\alpha^*$  is the equilibrium isotopic fractionation factor dependent on the temperature at the  
 256 evaporating surface. For oxygen

$$257 \quad \frac{1}{\alpha^*} = \exp(1137T_L^{-2} - 0.4256T_L^{-1} - 2.0667 \times 10^{-3}) \quad (4)$$

258 and for hydrogen

$$259 \quad \frac{1}{\alpha^*} = \exp(24844T_L^{-2} - 76.248T_L^{-1} - 52.61 \times 10^{-3}) \quad (5)$$

260 Where  $T_L$  is the temperature of the lake surface water in degrees Kelvin (Majoube 1971),  $h$  is  
 261 the relative humidity normalized to the saturation vapour pressure at the temperature of the air  
 262 water interface and  $\varepsilon_k$  is the kinetic fraction factor; for  $\delta^{18}\text{O}$ ,  $\varepsilon_k$  has been shown to approximate  
 263  $14.2(1 - h)$  and  $12.5(1 - h)$  for  $\delta^2\text{H}$  (Gonfiantini 1986).  $\delta_A$  is the isotopic value of the air  
 264 vapour over the lake and  $\varepsilon = \varepsilon^* + \varepsilon_k$  where  $\varepsilon^* = 1000(1 - \alpha^*)$ .

265 Gibson (2002) and Gibson et al. (2016) have shown that the relationship between  $\delta_P$   
 266 and  $\delta_A$  varies in different environmental settings, and advocate using a measured LEL, as we  
 267 have available here, to calculate the suitable regional  $\delta_P - \delta_A$  relationship.

268 Finally, we attempted to balance the hydrological and isotopic components of the Aweng  
269 Co lake system, to give estimates for each of the parameters in equation 1. Based on optimized  
270 values of  $c$  and  $g$ , and a constant groundwater inflow, and using average values for each  
271 modelled component from the 10 years of monitoring for which lake volumes were measured  
272 (Table 1, ESM 3) we undertook a mass balancing exercise, such that lake inputs should balance  
273 lake outputs (Lacey and Jones 2018), i.e.

$$274 P_L \delta_{PL} + R_i \delta_{Ri} + GMW \delta_G + G_i \delta_{Gi} = E \delta_E + G_o \delta_L \quad (6)$$

275 As all isotopic values are known, equation 6 can then be optimized, varying  
276 groundwater inputs such that the equation balances for both  $\delta^{18}\text{O}$  and  $\delta^2\text{H}$  values, resulting in  
277 estimates for the percentage contribution of each of these parameters to the Aweng Co  
278 hydrology.

279

## 280 **Results**

281

282 Changes in lake volume since the late 1990s

283

284 Between 1980 and 1999, lake area and lake volume of Aweng Co increased from 46.51 km<sup>2</sup> to  
285 60.69 km<sup>2</sup> and from 57.52 × 10<sup>6</sup> m<sup>3</sup> to 83.74 × 10<sup>6</sup> m<sup>3</sup>, respectively; with a rapid lake area  
286 expansion between 1996 ~ 1999 (Fig. 2d). Before 1999, lake area and lake volume increased  
287 slowly at 0.74 km<sup>2</sup> yr<sup>-1</sup> and 1.38 × 10<sup>6</sup> m<sup>3</sup> yr<sup>-1</sup>, respectively. After 1999 lake area and lake  
288 volume increased reaching 69.15 km<sup>2</sup> and 125.02 × 10<sup>6</sup> m<sup>3</sup> in 2002, and then decreased until  
289 2005; with an increase from 2006, culminating in 2008 with an area of 71.06 km<sup>2</sup> and a volume  
290 of 136.77 × 10<sup>6</sup> m<sup>3</sup>, respectively. The lake reached maximum size for the study period in 2010  
291 with an area of 71.67 km<sup>2</sup> and a volume of 153 × 10<sup>6</sup> m<sup>3</sup>, and then shrank a little (Fig. 2d, 2e).  
292 The lake area and lake volume increased at a rate of 0.998 km<sup>2</sup> yr<sup>-1</sup> and 6.29 × 10<sup>6</sup> m<sup>3</sup> yr<sup>-1</sup> from  
293 1999 to 2010.

294 Correlations (Fig. 3) between each known hydroclimate parameter and lake volume  
295 change show that precipitation and glacier melt water changes both have significant and  
296 positive correlations with lake volume change. Evaporation has a negative relationship with

297 lake volume change, but the relationship is relatively weak, and not significant.

298

299 Aweng Co Isotope Hydrology

300

301 Precipitation samples at Aweng Co (Fig. 4) lie on a local meteoric water line (MWL). Lake  
302 water samples lie to the right of the Aweng Co MWL, and with the groundwater sample describe  
303 a local evaporation line (LEL) with a gradient of 5.64 (Fig. 4).

304

305 Model Results

306

307 The results of initial optimization showed it is difficult to optimize  $r^2$ , slope and intercept  
308 concurrently (Table 2), and the best combination of  $c$ ,  $g$  and groundwater input, to give  
309 variability in the model at a magnitude that matches the measured volume changes is where  $c$   
310 and  $g$  are optimized to give a regression with slope of 1 (resulting in an  $r^2$  of 0.64) in which  
311 case a constant amount of groundwater inflow supplying the lake is required to give the 0  
312 intercept.

313 When calculating  $\delta_L$  for the “index lake” we used a lake system where  $\delta_E$  was equal to  
314 the intercept value of the LEL and Aweng Co MWL. In this case for  $\delta_L$ ,  $\delta_A$  and  $\delta_E$  to sit sensibly  
315 in  $\delta^{18}\text{O} - \delta\text{D}$  space (Fig. 4), an adjustment, via a constant ( $k$ ), is required to the standard  
316 equilibrium relationship between  $\delta_P$  and  $\delta_A$  (Gibson et al. 2016), where:

$$317 \delta_A = \frac{\delta_P - k\varepsilon^*}{1 + 10^{-3} \cdot k\varepsilon^*} \quad (7)$$

318 The value of  $k$  needed here (0.5), to fit the theoretical LEL to that measured in this study is  
319 typical for highly seasonal climates such as that at Aweng Co (Gibson et al. 2016).

320 The contributions of each component from the balanced  $\delta^{18}\text{O}$  and  $\delta^2\text{H}$  isotopic models  
321 (equation 6) are nearly the same (Table 3). Based on the  $\delta^{18}\text{O}$  balance model, the biggest  
322 supplier of water to Aweng Co is groundwater inflow, which accounts for 67 % and the smallest  
323 is glacier melt water that is 4 %. Precipitation and runoff in the catchment supply 10 % and 19 %  
324 to the hydrological systems, respectively. Evaporation accounts for 57 % of the water loss, more  
325 than the groundwater outflow, which is 43 %.

326

327 Sediment chronology and proxies

328

329 The dating model for the top of the core showed that the sediments at 14 cm depth were  
330 deposited ca. 1898 AD (ESM 4). We used the upper 7 cm of sediment in this study, which  
331 represented the time period since the late 1970s, with a sampling resolution of 0.5 cm (2.6  
332 years). The  $\delta^{18}\text{O}_{\text{carb}}$  values were around 1.5 ‰ between 1979 and 1984, and then decreased to  
333 0.34 ‰ in 1989 and kept relatively stable until 1997, followed by a trough (with a lowest  
334  $\delta^{18}\text{O}_{\text{carb}}$  value of  $-1.24$  ‰) around the mid-2000s and a positive trend after  $\sim 2007$  (Fig. 2g).

335

## 336 Discussion

337

338 Contributors to lake volume change: monitoring and modelling results

339

340 The combined monitoring and various modelling exercises for Aweng Co presented here have,  
341 at least on a general scale, begun to tell a coherent story for the lake system. The combined  
342 hydrological and isotope mass balance modelling (Table 3) give a similar picture to the water-  
343 isotope bi-plot (Fig. 4) in suggesting that both evaporation and groundwater are important  
344 outputs from the lake. The estimate of two thirds loss by evaporation (Table 3) is a sensible  
345 order of magnitude given the location of Aweng Co on the LEL (Fig. 4), the gradient of which  
346 is very similar to the LEL gradient (5.51) for other closed lakes that have experienced lake-  
347 expansions in recent decades on the Tibetan Plateau (Yuan et al. 2011). Correlations (Fig. 3)  
348 between each known hydroclimate parameter and lake volume change indicate both glacial melt  
349 water and changing precipitation amount could be controlling the observed lake area change.

350 To further refine our hydrological model we used the isotope hydrology of the site (Fig.  
351 4). Groundwater, isotopically, lies on the Aweng Co MWL, which has a similar gradient to the  
352 MWL described by Guo et al. (2017) for Ngari, 190 km far from Aweng Co and  $\sim 170$  m lower.  
353 If the groundwater is a mixture of both precipitation and glacial melt water, the isotope values  
354 of these different components could help to estimate the relative contributions of the two

355 sources. There are minimal data with which to undertake this exercise, but with that available  
356 we can make a preliminary estimate of the amount of precipitation and glacier melt water in the  
357 groundwater entering Aweng Co. The most negative of the precipitation samples collected in  
358 the 2015 field season ( $\delta^{18}\text{O} = -13.86 \text{ ‰}$ ;  $\delta^2\text{H} = -115.48 \text{ ‰}$ ) was a sample of snow, and  
359 therefore probably lies towards the negative isotopic end of local precipitation. There are no  
360 isotope data from the glacier that feeds Aweng Co, but  $\delta^{18}\text{O}$  values for other Tibetan glaciers  
361 are typically in the range of the catchment's snow sample. The average  $\delta^{18}\text{O}$  value from the  
362 Puruogangri Ice Cap is  $-13.66 \text{ ‰}$  in the most recent 50 years (Thompson et al. 2011), the upper  
363 meters of the Guliya Ice Cap, in the north of the plateau, and in a different climate region to  
364 Aweng Co, average  $-11.2 \text{ ‰}$  and  $-13.1 \text{ ‰}$  from the 2015 and 1992 cores respectively  
365 (Thompson et al. 2018). Given these values, and the groundwater sample ( $\delta^{18}\text{O} = -12.29 \text{ ‰}$ ,  
366  $\delta^2\text{H} = -99.77 \text{ ‰}$ ), it appears likely that this groundwater is dominated in composition by snow  
367 and glacier melt water ( $\sim 70 \%$ ), although distinguishing between these two would need further  
368 monitoring of the Aweng Co system. It is also possible that our precipitation values and runoff  
369 constant underestimate the amount of snowmelt that enters the lake, such that our "groundwater"  
370 value here includes all currently unmeasured inflows, including snow melt.

371 For the differing inflow parameters, given the location of the groundwater sample and  
372 average precipitation in  $\delta^{18}\text{O}$   $\delta^2\text{H}$  space (Fig. 4), if  $\sim 70 \%$  of the "groundwater" inflow comes  
373 from ice and snow melt, then approximately 50 % of Aweng Co inflow (surface and  
374 groundwater) comes from ice and snowmelt and 50 % from summer rainfall. This would  
375 suggest that for this lake system both glacier melt and rainfall changes may help to explain  
376 recent lake area expansion.

377 One potential way to distinguish further which component may have been more  
378 significant in recent times is to look at the potential sensitivity of the system to changes in these  
379 different parameters. Although there is a strong correlation between precipitation and lake  
380 volume change (Fig. 3) the magnitude of lake area and lake volume change through the time  
381 period of this correlation (1999-2009) is small compared to the longer term variability (Fig. 2).  
382 Over the longer period since  $\sim 1980$  there have been larger increases in lake area, but no similar  
383 trend in increasing annual precipitation.

384 There are relatively few data points to observe the relationship between lake area and  
385 glacier area, as a proxy for melt water, through the 1999-2009 window, but the significant  
386 decline in glacier area between 1997 and 1999 matches the significant period of lake area  
387 expansion which, alongside the lack of significant shifts in precipitation trends through that  
388 time period, suggests that it was glacier melt water which drove the change in lake volume.

389 The analyses presented here suggest that isotope hydrology can help further the  
390 understanding of controls on changes in western Tibetan lakes, but that to fully exploit their  
391 potential a more detailed monitoring programme needs to be undertaken, ideally over a number  
392 of years.

393

394  $\delta^{18}\text{O}_{\text{carb}}$  evidence

395

396 The variation of  $\delta^{18}\text{O}_{\text{carb}}$  is controlled by lake water  $\delta^{18}\text{O}$  and temperature changes (Leng and  
397 Marshall 2004; Xu et al. 2006), and therefore the signals of lake hydrology variations could be  
398 preserved in the  $\delta^{18}\text{O}_{\text{carb}}$  sediment record. The mean summer temperature change rise of  $1.1^\circ\text{C}$   
399 (Fig. 2b) would lead to  $\delta^{18}\text{O}_{\text{carb}}$  change of  $\sim 0.26\text{‰}$  based on a temperature-dependence of  
400 carbonate fractionation of  $-0.24\text{‰}/^\circ\text{C}$  (Craig 1965), which is not enough to explain the  
401 magnitude of  $\delta^{18}\text{O}_{\text{carb}}$  fluctuations ( $1.74\text{‰}$ ) between 1997 and 2006 (Fig. 2g; ESM 5),  
402 suggesting that changes in lake water  $\delta^{18}\text{O}$  have been important in driving the recorded  $\delta^{18}\text{O}_{\text{carb}}$ .  
403 This, alongside the importance of evaporation in the lake system (Fig. 4) suggests that the  
404 inflow to evaporation ratio (I:E) is probably the main driver of  $\delta^{18}\text{O}_{\text{carb}}$  at Aweng Co. Of  
405 particular interest through recent decades is the negative excursion in  $\delta^{18}\text{O}_{\text{carb}}$  between  $\sim 1999$   
406 and  $\sim 2008$ , which would need an increase in inflow or decrease in evaporation in an I:E driven  
407 system, or a significant change in the isotopic component of the inflowing water.

408 During the period 1999 to 2007, evaporation at the lake surface showed an overall slight  
409 increasing trend (Fig. 2c), with only a short, two year, reduction in evaporation through that  
410 time. Even within the chronological uncertainties of the core record, this is not enough to  
411 explain the trends in the  $\delta^{18}\text{O}_{\text{carb}}$  record.

412 Comparison of trends in precipitation (Fig. 2a) with the  $\delta^{18}\text{O}_{\text{carb}}$  record also shows no

413 clear relationship between periods of increased amounts of precipitation and negative isotope  
414 excursions. The biggest decline in glacier area in the late 1990s does match, within the  
415 chronological errors of the core, the  $\delta^{18}\text{O}_{\text{carb}}$  shift to more negative values ( $-1.24$  ‰ in 2006).  
416 Given I:E ratio is likely the main driver of  $\delta^{18}\text{O}_{\text{carb}}$  change, an increased amount of glacier melt  
417 water would increase lake area/volume and lead to a negative shift in  $\delta^{18}\text{O}_{\text{carb}}$ .

418 Although the  $\delta^{18}\text{O}_{\text{carb}}$  returns to early 1990s values ( $\sim 0.5$  ‰) after the negative excursion  
419 towards the top of the core (Fig. 2), there are no similar returns for either the glacier area or  
420 the lake area. One interpretation for the difference is that the lake isotope values are returning  
421 to a steady state following the negative excursion, but these isotope values are similar to those  
422 when the lake level was lower. This could be because inflows and outflows to the system are  
423 generally the same in both the low and high lake level status. In such a system, flux, which  
424 has been considered important in controlling  $\delta^{18}\text{O}_{\text{carb}}$  in other lake systems (Jones et al. 2007),  
425 remains the same, while volume has increased due to the elevated glacial melt water period in  
426 the late 1990s. In this scenario it is also possible that the negative excursion under discussion  
427 is a result of the particularly negative isotopic value of that glacial melt water, rather than the  
428 amount of it, such that the impact of this input changed the  $\delta^{18}\text{O}_{\text{carb}}$  record more than the  
429 volume change. Meanwhile, the duration of the isotopic impact was limited by the relatively  
430 short residence time of the water, with negative isotopic water flushed through the system,  
431 whilst lake volume remains relatively unchanged. Overall, it is likely that a combined effect  
432 of increased inflow of particularly isotopically-negative glacial melt water led to this negative  
433 shift in  $\delta^{18}\text{O}_{\text{carb}}$ .

434 This comparison exercise shows how even with instrumental data available for contrast,  
435 the interpretation of  $\delta^{18}\text{O}_{\text{carb}}$  records is complicated by the multiple potential controls that can  
436 lead to an abrupt change in a core  $\delta^{18}\text{O}_{\text{carb}}$  record. This highlights the need to have multiple  
437 proxies from which more robust interpretations of environmental changes from down-core data  
438 can be made beyond the instrumental time period.

439  $\delta\text{D}$

## 440 **Conclusions**

441

442 The combined monitoring, modelling and palaeolimnological approach taken here shows the  
443 potential for  $\delta^{18}\text{O}_{\text{carb}}$  to be used to investigate lake area change in the western Tibetan Plateau,  
444 whilst highlighting the complexities of the system. This understanding is important for using  
445 such core records to reconstruct longer term environmental change in the region. Both the  
446 monitoring, modelling and  $\delta^{18}\text{O}_{\text{carb}}$  evidence point to the importance of glacial melt water in  
447 influencing the lake area and isotopic record of Aweng Co, but highlight that the sensitivities  
448 of these two parts of the lake system to glacial melt water change can be different. The flux of  
449 water through the lake system, controlled by precipitation amount and evaporation as well as  
450 glacial melt water, is also therefore important in driving the resulting  $\delta^{18}\text{O}_{\text{carb}}$  record preserved  
451 in the sediments, and the dominant hydrological controls may change through time.

452

### 453 **Acknowledgments**

454

455 This study is supported by the National Natural Science Foundation of China (NSFC 41771212)  
456 and Fundamental Research Fund for the Central Universities (lzujbky-2017-it81). We would  
457 like to thank Juzhi Hou, Mingda Wang, Yaping Yang and Erlei Zhu for assisting the field work.  
458 We also thank Melanie Leng for her constructive suggestions in improving the quality of the  
459 manuscript, and Xian Wu for providing the interpolated meteorological data in the catchment.  
460 We thank Thomas J. Whitmore, Steffen Mischke and two anonymous reviewers for detailed  
461 comments which improved the manuscript. The authors have no conflict of interest to declare.

462

### 463 **References**

464

- 465 Appleby PG, Oldfield F (1978) The calculation of lead-210 dates assuming a constant rate of supply of  
466 unsupported  $^{210}\text{Pb}$  to the sediment. *Catena* 5:1–8
- 467 Atkinson SE, Woods RA, Sivapalan M (2002) Climate and landscape controls on water balance model complexity  
468 over changing timescales. *Water Resour Res* 38:50-1–50-15
- 469 Chen J, Zhu X, Vogelmann JE, Gao F, Jin S (2011) A simple and effective method for filling gaps in Landsat ETM  
470 + SLC-off images. *Remote Sens Environ* 115:1053–1064
- 471 Conway D (1997) A water balance model of the Upper Blue Nile in Ethiopia. *Hydrol Sci J* 42:165–286
- 472 Craig H (1965) The measurement of oxygen isotope palaeotemperatures. In: Tongiorgi E (ed) *Stable isotopes in*  
473 *oceanographic studies and palaeotemperatures*. Consiglio Nazionale delle Ricerche Laboratorio di Geologia  
474 Nucleare, Pisa, pp 161–182
- 475 Craig H, Gordon LI (1965) Deuterium and oxygen-18 variation in the ocean and marine atmosphere. In: Tongiorgi



476 E (ed) Stable isotopes in oceanography studies and paleotemperatures. Consiglio Nazionale delle Ricerche  
477 Laboratorio di Geologia Nucleare, Pisa, pp 9-130

478 Crétau JF, Abarca-del-Río R, Bergé-Nguyen M, Arsen A, Drolon V, Clos G, Maisongrande P (2016) Lake volume  
479 monitoring from space. *Surv Geophys* 37:269–305

480 Gibson J (2002) A new conceptual model for predicting isotopic enrichment of lakes in seasonal climates. Pages  
481 *News* 10:10–11

482 Gibson JJ, Birks SJ, Yi Y (2016) Stable isotope mass balance of lakes: a contemporary perspective. *Quat Sci Rev*  
483 131:316–328

484 Gleick PH (1987) The development and testing of a water balance model for climate impact assessment: modeling  
485 the Sacramento Basin. *Water Resour Res* 23:1049–1061

486 Gonfiantini R (1986) Environmental isotopes in lake studies. In: Fritz P, Fontes J C (eds) *Handbook of*  
487 *Environmental Isotope Geochemistry*. vol 3. Elsevier Scientific Publishing Company, Amsterdam, pp 113-  
488 168

489 Guo S, Wang J, Xiong L, Ying A, Li D (2002) A macro-scale and semi-distributed monthly water balance model  
490 to predict climate change impacts in China. *J Hydrol* 268:1–15

491 Guo X, Tian L, Wen R, Yu W, Qu D (2017) Controls of precipitation  $\delta^{18}\text{O}$  on the northwestern Tibetan Plateau: A  
492 case study at Ngari station. *Atmos Res* 189:141–151

493 Huss M (2013) Density assumptions for converting geodetic glacier volume change to mass change. *The*  
494 *Cryosphere*, 7(3):877-887

495 Jones MD, Cuthbert MO, Leng MJ, McGowan S, Mariethoz G, Arrowsmith C, Sloane HJ, Humphrey KK, Cross  
496 I (2016) Comparisons of observed and modelled lake  $\delta^{18}\text{O}$  variability. *Quat Sci Rev* 131:329–340

497 Jones MD, Roberts CN, Leng MJ (2007) Quantifying climatic change through the last glacial-interglacial transition  
498 based on lake isotope palaeohydrology from central Turkey. *Quat Res* 67:463–473

499 Lacey JH, Jones MD (2018) Quantitative reconstruction of early Holocene and last glacial climate on the Balkan  
500 Peninsula using coupled hydrological and isotope mass balance modelling. *Quat Sci Rev* 202:109–121

501 Lei Y, Yang K, Wang B, Sheng Y, Bird BW, Zhang G, Tian L (2014) Response of inland lake dynamics over the  
502 Tibetan Plateau to climate change. *Clim Change* 125:281–290

503 Lei Y, Yao T, Bird BW, Yang K, Zhai J, Sheng Y (2013) Coherent lake growth on the central Tibetan Plateau since  
504 the 1970s: Characterization and attribution. *J Hydrol* 483:61–67

505 Lei Y, Yao T, Yang K, Sheng Y, Kleinherenbrink M, Yi S, Bird BW, Zhang X, Zhu L, Zhang G (2017) Lake  
506 seasonality across the Tibetan Plateau and their varying relationship with regional mass changes and local  
507 hydrology. *Geophys Res Lett* 44:892–900

508 Leng MJ, Marshall JD (2004) Palaeoclimate interpretation of stable isotope data from lake sediment archives.  
509 *Quat Sci Rev* 23:811–831

510 Li X, Wang M, Zhang Y, Lei L, Hou J (2017) Holocene climatic and environmental change on the western Tibetan  
511 Plateau revealed by glycerol dialkyl glycerol tetraethers and leaf wax deuterium-to-hydrogen ratios at Aweng  
512 Co. *Quat Res* 87:455–467

513 Linacre E (1992) *Climate data and resources: a reference and guide*. Routledge, London, pp 366

514 Magny M (2004) Holocene climate variability as reflected by mid-European lake-level fluctuations and its  
515 probable impact on prehistoric human settlements. *Quat Int* 113:65–79

516 Majoube F (1971) Fractionnement en oxygene-18 et en deuterium entre l'eau et sa vapeur. *J Chem Phys* 68: 1423–  
517 1436

518 Neckel N, Kropáček J, Bolch T, Hochschild V (2014) Glacier mass changes on the Tibetan Plateau 2003-2009  
519 derived from ICESat laser altimetry measurements. *Environ Res Lett* 9:1–7

- 520 Phan VH, Lindenbergh R, Menenti M (2012) ICESat derived elevation changes of Tibetan lakes between 2003  
521 and 2009. *Int J Appl Earth Obs Geoinf* 17:12–22
- 522 Qiang M, Song L, Chen F, Li M, Liu X, Wang Q (2013) A 16-ka lake-level record inferred from macrofossils in a  
523 sediment core from Genggahai Lake, northeastern Qinghai-Tibetan Plateau (China). *J Paleolimnol* 49:575–  
524 590
- 525 Rouse WR (1998) A water balance model for subarctic sedge fen and its application to climatic change. *Clim*  
526 *Change* 38: 207–234
- 527 Rowe HD, Guilderson TP, Dunbar RB, Southon JR, Seltzer GO, Mucciarone DA, Fritz SC, Baker PA (2003) Late  
528 Quaternary lake-level changes constrained by radiocarbon and stable isotope studies on sediment cores from  
529 Lake Titicaca, South America. *Glob Planet Change* 38:273–290
- 530 Song C, Huang B, Richards K, Ke L, Phan VH (2014) Accelerated lake expansion on the Tibetan Plateau in the  
531 2000s: Induced by glacial melting or other processes? *Water Resour Res* 50:3170–3186
- 532 Song C, Huang B, Ke L (2013) Modeling and analysis of lake water storage changes on the Tibetan Plateau using  
533 multi-mission satellite data. *Remote Sens Environ* 135:25–35
- 534 Steinman BA, Rosenmeier MF, Abbott MB (2010a) The isotopic and hydrologic response of small, closed-basin  
535 lakes to climate forcing from predictive models: Simulations of stochastic and mean-state precipitation  
536 variations. *Limnol Oceanogr* 55:2246–2261
- 537 Steinman BA, Rosenmeier MF, Abbott MB, Bain DJ (2010b) The isotopic and hydrologic response of small,  
538 closed-basin lakes to climate forcing from predictive models: Application to paleoclimate studies in the  
539 upper Columbia River basin. *Limnol Oceanogr* 55:2231–2245
- 540 Thompson LG, Mosley-Thompson E, Davis ME, Brecher HH (2011) Tropical glaciers, recorders and indicators  
541 of climate change, are disappearing globally. *Ann Glaciol* 52:23–34
- 542 Thompson LG, Yao T, Davis ME, Mosley-Thompson E, Wu G, Porter SE, Xu B, Lin PN, Wang N, Beauson E,  
543 Duan K, Sierra-Hernandez MR, Kenny DV (2018) Ice core records of climate variability on the Third Pole  
544 with emphasis on the Guliya ice cap, western Kunlun Mountains. *Quat Sci Rev* 188:1–14
- 545 Wang S, Dou H (1998) Records of lakes in China (in Chinese). Science Press, Beijing
- 546 Wu X, Huang W, Chen F (2014) Construction and application of monthly air temperature and precipitation gridded  
547 datasets with high resolution (0.025\*0.025) over China during 1951-2012 (in Chinese). *J Lanzhou*  
548 *University* 50:213–220
- 549 Xu H, Ai L, Tan L, An Z (2006) Stable isotopes in bulk carbonates and organic matter in recent sediments of Lake  
550 Qinghai and their climatic implications. *Chem Geol* 235:262–275
- 551 Xu H, Goldsmith Y, Lan J, Tan L, Wang X, Zhou X, Cheng J, Lang Y, Liu C (2020) Juxtaposition of western  
552 Pacific subtropical high on Asian summer monsoon shapes subtropical East Asian precipitation. *Geophys*  
553 *Res Lett* 47:1–10
- 554 Yang K, Wu H, Qin J, Lin C, Tang W, Chen Y (2014) Recent climate changes over the Tibetan Plateau and their  
555 impacts on energy and water cycle: A review. *Glob Planet Change* 112:79–91
- 556 Yang M, Nelson FE, Shiklomanov NI, Guo D, Wan G (2010) Permafrost degradation and its environmental effects  
557 on the Tibetan Plateau: A review of recent research. *Earth Sci Rev* 103:31–44
- 558 Yao T, Pu J, Lu A, Wang Y, Yu W (2007) Recent glacial retreat and its impact on hydrological processes on the  
559 Tibetan Plateau, China, and surrounding regions. *Arctic Antarct Alp Res* 39:642–650
- 560 Yao T, Thompson L, Yang W, Yu W, Gao Y, Guo X, Yang X, Duan, K, Zhao, H, Xu B, Pu J, Lu A, Xiang Y, Kattel  
561 DB, Joswiak D (2012) Different glacier status with atmospheric circulations in Tibetan Plateau and  
562 surroundings. *Nat Clim Change* 2:663–667
- 563 Yuan F, Sheng Y, Yao T, Fan C, Li J, Zhao H, Lei Y (2011) Evaporative enrichment of oxygen-18 and deuterium

564 in lake waters on the Tibetan Plateau. *J Paleolimnol* 46:291–307

565 Zhang G (2019) The lakes larger than 1 km<sup>2</sup> in Tibetan Plateau (V2.0) (1970s-2018). Natl Tibet Plateau Data Cent

566 Zhang G, Li J, Zheng G (2017b) Lake-area mapping in the Tibetan Plateau: an evaluation of data and methods. *Int*

567 *J Remote Sens* 38:742–772

568 Zhang Y, Li Y, Zhu G (2019b) The effect of altitude on temperature, precipitation and climatic zone in the Qinghai-

569 Tibetan (in Chinese). *J Glaciol Geocryol* 41:505–515

570 Zhang G, Luo W, Chen W, Zheng G (2019a) A robust but variable lake expansion on the Tibetan Plateau. *Sci Bull*

571 64:1306-1309

572 Zhang G, Xie H, Kang S, Yi D, Ackley SF (2011) Monitoring lake level changes on the Tibetan Plateau using

573 ICESat altimetry data (2003 – 2009). *Remote Sens Environ* 115:1733–1742

574 Zhang G, Yao T, Piao S, Bolch, T, Xie H, Chen D, Gao Y, O’Reilly CM, Shum CK, Yang K, Yi S, Lei Y, Wang W,

575 He Y, Shang K, Yang X, Zhang H (2017a) Extensive and drastically different alpine lake changes on Asia’s

576 high plateaus during the past four decades. *Geophys Res Lett* 44:252–260

577 Zhang G, Yao T, Xie H, Wang W, Yang W (2015) An inventory of glacial lakes in the Third Pole region and their

578 changes in response to global warming. *Glob Planet Change* 131:148–157

579 Zhang G, Yao T, Xie H, Zhang K, Zhu F (2014) Lakes’ state and abundance across the Tibetan Plateau. *Chin Sci*

580 *Bull* 59:3010–3021

581 Zhu L, Xie M, Wu Y (2010) Quantitative analysis of lake area variations and the influence factors from 1971 to

582 2004 in the Nam Co basin of the Tibetan Plateau. *Chi Sci Bull* 55:1294–1303

583

584 **Tables**

585

586 **Table 1** Annual values for the parameters of the water balance model from 10/1999 to 10/2009.

587  $P_L$  is the precipitation on the lake surface (Wu et al. 2014).  $S_L$  is the lake surface area (average

588 of the area at the start and end of the time period).  $S_C$  is the area of catchment excluding the

589 lake area.  $E_L$  is the evaporation from the lake surface. LVC is the lake volume change in each

590 period

start	end	$P_L$ (mm)	$S_L$ (m <sup>2</sup> )	$S_C$ (m <sup>2</sup> )	$E_L$ (mm)	LVC (m <sup>3</sup> )
10/1999	10/2000	199	63897313	1988402687	916	27017800
10/2000	10/2001	165	67175062	1985124938	979	1161000
10/2001	10/2002	205	68197610	1984102390	914	13097000
10/2002	10/2003	149	68967180	1983332820	886	-10094000
10/2003	10/2004	130	67938056	1984361944	997	-5669000
10/2004	10/2005	159	66809354	1985490647	942	-2652000
10/2005	10/2006	166	67833813	1984466187	962	21009000
10/2006	10/2007	157	69168096	1983131905	984	384000
10/2007	10/2008	205	70129135	1982170865	975	8777000
10/2008	10/2009	125	70121542	1982178458	1006	-14563000

591

592

593

594

595

596

597

598

599

600

601

602

603

604

605

606

607

608

609

610

611

612 **Table 2** The results of changing model constants  $c$  and  $g$  to optimize  $r^2$ , slope and intercept of  
 613 the relationship between known and modelled  $\Delta V_L$

Constant $c$	Constant $g$	$r^2$	slope	intercept
0.06	0.13	0.64	1.00	31,493,754
0.09	0.94	0.51	0.28	15
0.84	0.74	0.68	0.17	-38,453,042

614  
 615  
 616  
 617  
 618  
 619  
 620  
 621  
 622  
 623  
 624  
 625  
 626  
 627  
 628  
 629  
 630  
 631  
 632  
 633  
 634  
 635  
 636  
 637

638 **Table 3** Estimates of contributions of different hydrological components of the Aweng Co  
 639 system from the isotope mass balance calculation (Equation 6)

640

	Hydrological Component	Contribution (%)	
		from $\delta^{18}\text{O}$ balance	from $\delta^2\text{H}$ balance
<b>Water input</b>	P <sub>L</sub>	10	11
	R <sub>C</sub>	19	20
	GMW	4	5
	G <sub>I</sub>	67	65
<b>Water output</b>	E	57	61
	G <sub>O</sub>	43	39

641

642

643

644

645

646

647

648

649

650

651

652

653

654

655

656

657

658

659

660

661

662

663

664

665

666

667

668

669

670 **Figure captions**

671

672 **Fig.1** The location of Aweng Co (a), the topography of Aweng Co catchment (b) and the monthly mean  
673 temperature and total monthly precipitation at Shiquanhe Station (c). The boundary of the inner TP (a) was  
674 defined according to Zhang et al. (2015).

675

676 **Fig. 2** Comparisons of lake area change and glacier area change with  $\delta^{18}\text{O}_{\text{carb}}$  value, and meteorological data.  
677 (a) Interpolated precipitation in the Aweng Co catchment from 1980 to 2012 (Wu et al. 2014). (b) Interpolated  
678 mean summer temperature (June to August) in the Aweng Co catchment from 1980 to 2012 (Wu et al. 2014).  
679 (c) Calculated evaporation on the lake surface from May to September in the Aweng Co catchment. (d) Aweng  
680 Co lake area since 1979. (e) Calculated lake volume. (f) Glacier area change from 1996 to 2010. (g)  
681 Sedimentary record  $\delta^{18}\text{O}_{\text{carb}}$  from Aweng Co from 1978 to 2014 (The data of  $\delta^{18}\text{O}_{\text{carb}}$  are shown in ESM 5).  
682 The black dots and bars represent the chronology of the samples and the errors (full data presented in ESM  
683 4).

684

685 **Fig. 3** The linear correlation between each parameter (left to right: precipitation on the lake surface;  
686 evaporation on the lake surface and glacier melt water) and lake volume change.  $P_L$  represents precipitation  
687 on the lake surface.  $S_L$  represents lake surface area.  $E_L$  represents evaporation on the lake surface.

688

689 **Fig. 4**  $\delta^{18}\text{O}$  vs.  $\delta^2\text{H}$  of different waters from Aweng Co. Blue dots are lake water from Aweng Co. Green  
690 Rhombus is the groundwater from the Aweng Co basin. Light blue crosses are lake water isotopes from the  
691 western Tibetan Plateau (Yuan et al. 2011). Small and large dark blue triangles are sampled precipitation and  
692 mean precipitation in the Aweng Co region respectively. Yellow triangle is the estimated isotopic value of the  
693 air vapour over the lake, black cross is the isotope value of the calculated evaporation from the lake surface,  
694 orange square is the calculated regional index lake (see text for details). MWL is the meteoric water line from  
695 Ngari station (Guo et al. 2017). Aweng Co MWL is the local meteoric water line. LEL is the local evaporation  
696 line. The isotope data used in this study are shown in ESM 5.

697

698

699

700

701

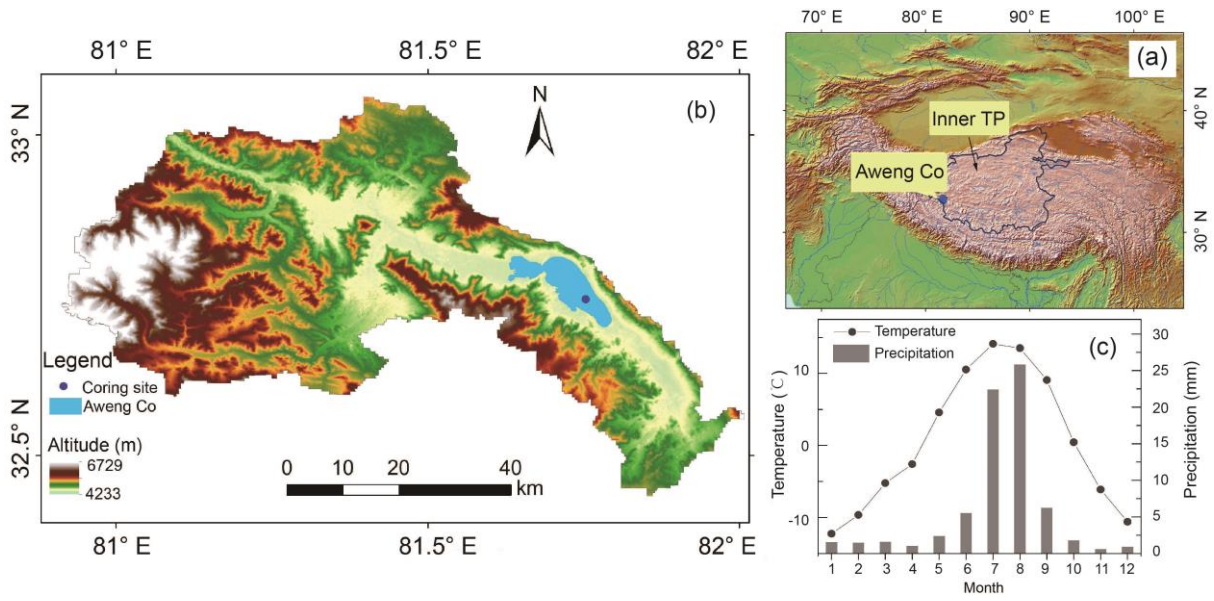
702

703 **Figures**

704

705 Fig. 1

706



707

708

709

710

711

712

713

714

715

716

717

718

719

720

721

722

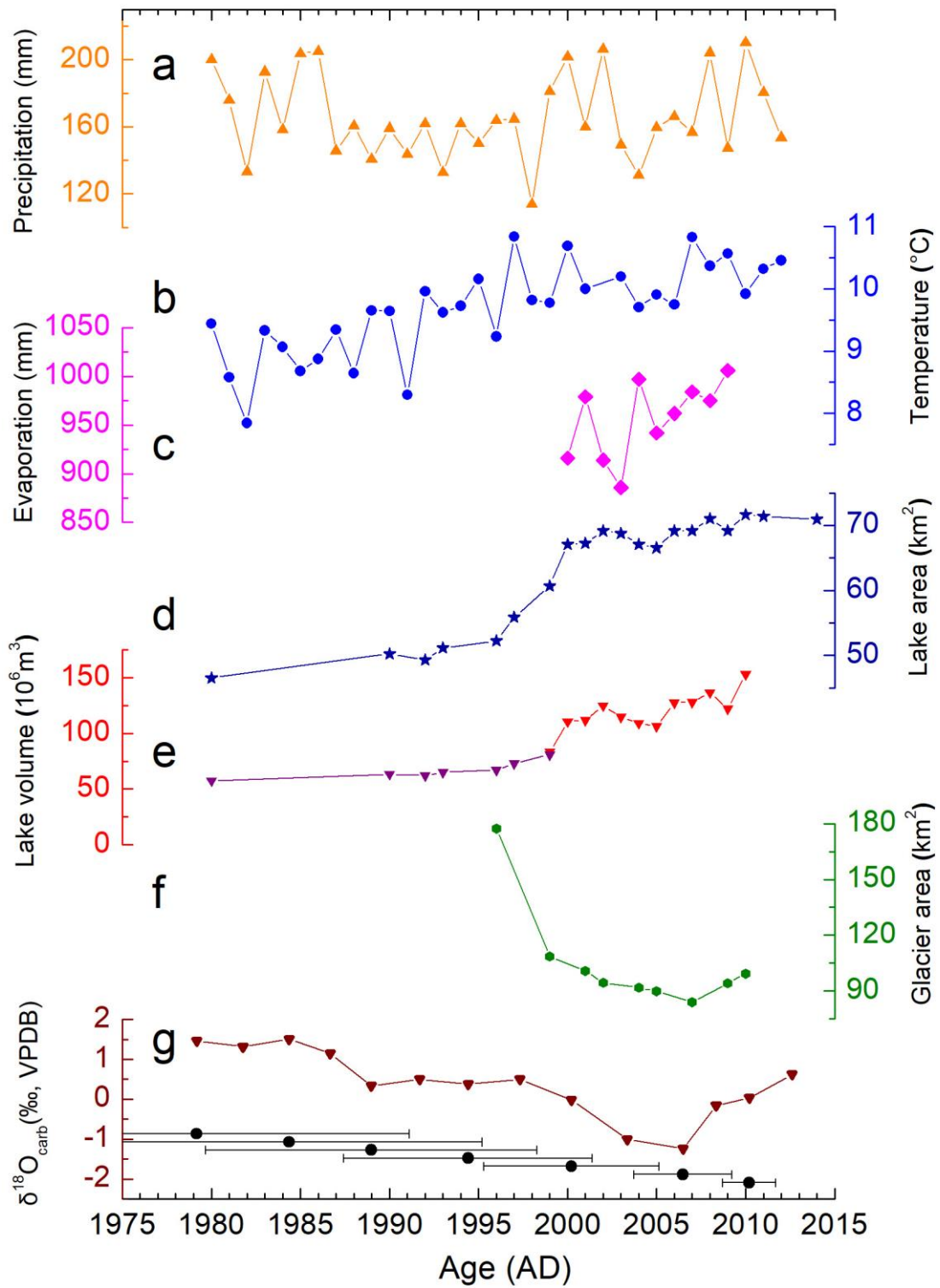
723

724



725 Fig. 2

726



727

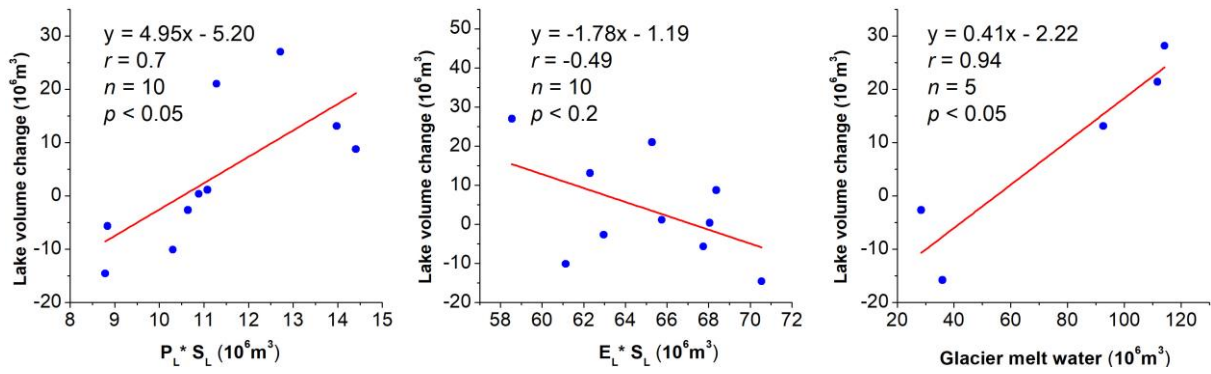
728

729

730

731 Fig. 3

732



733

734

735

736

737

738

739

740

741

742

743

744

745

746

747

748

749

750

751

752

753

754

755

756

757

758

759

760

761

762

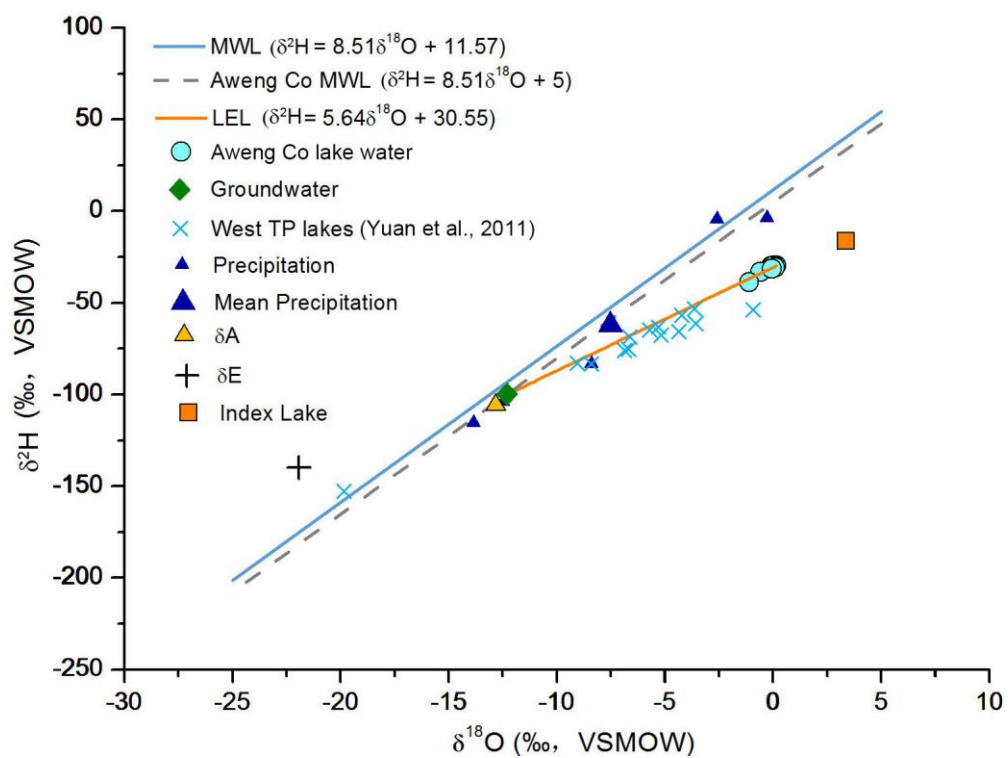
763

764

765

766  
767  
768  
769

Fig. 4



770